5-2019

Exploring the Electrical Properties of Twisted Bilayer Graphene

William Shannon
Linfield College

Exploring the Electrical Properties of Twisted Bilayer Graphene

William Shannon

A THESIS

Presented to the Department of Physics
LINFIELD COLLEGE
McMinnville, Oregon

In partial fulfillment of the requirements
for the Degree of

BACHELOR OF SCIENCE

May, 2019

THESIS COPYRIGHT PERMISSIONS

Please read this document carefully before signing. If you have questions about any of these permissions, please contact the DigitalCommons Coordinator.

Title of the Thesis:

Exploring the Electrical Properties of Twisted Bilayer Graphene

Author's Name: (Last name, first name)

Shannon, William

Advisor's Name

Dr. Jennifer Heath

DigitalCommons@Linfield (DC@L) is our web-based, open access-compliant institutional repository for digital content produced by Linfield faculty, students, staff, and their collaborators. It is a permanent archive. By placing your thesis in DC@L, it will be discoverable via Google Scholar and other search engines. Materials that are located in DC@L are freely accessible to the world; however, your copyright protects against unauthorized use of the content. Although you have certain rights and privileges with your copyright, there are also responsibilities. Please review the following statements and identify that you have read them by signing below. Some departments may choose to protect the work of their students because of continuing research. In these cases, the project is still posted in the repository but content will only be accessible by individuals who are part of the Linfield community.

CHOOSE THE STATEMENT BELOW THAT DEFINES HOW YOU WANT TO SHARE YOUR THESIS. THE FIRST STATEMENT PROVIDES THE MOST ACCESS TO YOUR WORK; THE LAST STATEMENT PROVIDES THE LEAST ACCESS. CHOOSE ONLY ONE STATEMENT.

X I **agree** to make my thesis available to the Linfield College community and to the larger scholarly community upon its deposit in our permanent digital archive, DigitalCommons@Linfield, or its successor technology. My thesis will also be available in print at Nicholson Library and can be shared via interlibrary loan.

OR

_____ I **agree** to make my thesis available **only** to the Linfield College community upon its deposit in our permanent digital archive, DigitalCommons@Linfield, or its successor technology. My thesis will also be available in print at Nicholson Library and can be shared via interlibrary loan.

OR

_____ I **agree** to make my thesis available in print at Nicholson Library, including access for interlibrary loan.

OR

_____ I **agree** to make my thesis available in print at Nicholson Library only.

Updated April 25, 2018

NOTICE OF ORIGINAL WORK AND USE OF COPYRIGHT-PROTECTED MATERIALS:

If your work includes images that are not original works by you, you must include permissions from the original content provider or the images will not be included in the repository. If your work includes videos, music, data sets, or other accompanying material that is not original work by you, the same copyright stipulations apply. If your work includes interviews, you must include a statement that you have the permission from the interviewees to make their interviews public. For information about obtaining permissions and sample forms, see https://copyright.columbia.edu/basics/permissions-and-licensing.html.

NOTICE OF APPROVAL TO USE HUMAN OR ANIMAL SUBJECTS:

If your research includes human subjects, you must include a letter of approval from the Linfield Institutional Review Board (IRB); see https://www.linfield.edu/faculty/irb.html for more information. If your research includes animal subjects, you must include a letter of approval from the Linfield Animal Care & Use Committee.

NOTICE OF SUBMITTED WORK AS POTENTIALLY CONSTITUTING AN EDUCATIONAL RECORD UNDER FERPA:

Under FERPA (20 U.S.C. § 1232g), this work may constitute an educational record. By signing below, you acknowledge this fact and expressly consent to the use of this work according to the terms of this agreement.

BY SIGNING THIS FORM, I ACKNOWLEDGE THAT ALL WORK CONTAINED IN THIS PAPER IS ORIGINAL WORK BY ME OR INCLUDES APPROPRIATE CITATIONS AND/OR PERMISSIONS WHEN CITING OR INCLUDING EXCERPTS OF WORK(S) BY OTHERS.

IF APPLICABLE, I HAVE INCLUDED AN APPROVAL LETTER FROM THE IRB TO USE HUMAN SUBJECTS OR FROM ANIMAL CARE & USE TO USE ANIMAL SUBJECTS.

Signature Signature redacted Date 5/15/2019

Printed Name William D. Shannon

Approved by Faculty Advisor Signature redacted Date 5/15/2019

Updated April 25, 2018

Thesis Acceptance

Linfield College

Thesis Title: Exploring the Electrical Properties of Twisted Bilayer Graphene

Submitted by: William Shannon

Date Submitted: May, 2019

Research Advisor: Signature redacted

Dr. Heath

Thesis Advisor: Signature redacted

Dr. Crosser

Physics Department: Signature redacted

Dr. Murray

ABSTRACT

Exploring the Electrical Properties of Twisted Bilayer Graphene

Two-dimensional materials exhibit properties unlike anything else seen in conventional substances. Electrons in these materials are confined to move only in the plane. In order to explore the effects of these materials, we have built apparatus and refined procedures with which to create two-dimensional structures. Two-dimensional devices have been made using exfoliated graphene and placed on gold contacts. Their topography has been observed using Atomic Force Microscopy (AFM) confirming samples with monolayer, bilayer, and twisted bilayer structure. Relative work functions of each have been measured using Kelvin Probe Force Microscopy (KPFM) showing that twisted bilayer graphene has a surface potential 20 mV higher than that of monolayer graphene and 35 mV below bilayer graphene.

For my mother, who supported me in every possible way.

Contents

List of Figures

Chapter 1

Introduction

We live in a three-dimensional world. Everything we interact with has length, width, and height. Some things might be thin enough for us to consider them to be essentially "two-dimensional" such as sheets of paper, but an electron living in this paper would consider it to be massively thick. Indeed, making a truly two-dimensional structure in our world is impossible. The building blocks of our world, atoms, have a volume, meaning that everything will necessarily occupy some three-dimensional space. However, that did not stop scientists from trying to get as close as possible.

The idea of a material being only one atom thick has been around for quite some time. Since the 1940's people have theorized that it could be possible to create a stable structure with a thickness of only one atom. One of the first of these materials though to be a candidate for being "two-dimensional" was graphite.

While you may not recognize the name, graphite is a material that most people have probably used in their life, as it makes up the lead used in pencils. As you write with a pencil, layers of the graphite crystal flake off and remain behind on the paper to leave a visible mark. The crystal structure of graphite and its ability to sheer off into layers made it a prime candidate for being refined down to atomic thickness.

The problem was trying to determine how best to actually create the single atom thick lattice. It is not as easy as taking a sharp knife to a piece of graphite and

cutting off a slice. The required layer is so thin that no conventional method could be used to create it. In the end, an unexpected tool because the key to creating these two-dimensional materials, Scotch Tape. [1] By placing a flake of graphite on a piece of tape and repeatedly folding it back and forth one can slowly sheer off layer by layer of graphite until you create an atomically flat surface which bonds more strongly to a substrate than its neighboring layer.

Indeed, in 2004 Andre Geim and Konstantin Novoselov won the Nobel Prize in physics for the synthesis of graphene using this method. [1] Graphene is a hexagonal honeycomb lattice of carbon atoms only one layer thick. While bulk graphite is a relatively weak material prone to breaking along crystal planes, graphite is the strongest material ever created by man. [2] The electrical properties of graphene are also different than those of graphite. In graphene, electrons are free to move in three-dimensions, while in graphite they are only free to move in two. They are both, however, conductors. [3] In fact, this is certainly not the only interesting thing about two-dimensional materials.

The unique electric properties of these materials lead to exciting conclusions that have never been seen before in conventional materials. For example, a stack of two graphene layers twisted relative to one another can enter a superconducting state which is absent in the individual graphene layers. [4] Superconductivity is something that has only been observed in certain three-dimensional materials at extremely low temperature, so this new two-dimensional form of superconductivity demonstrates a new property that once fully understood could revolutionize electronics.

However, before we are able to create the next generation of super-conductive graphene devices, preliminary research needs to be done. Similarly to how doctors start by learning how each individual system in the human body works before developing new medicines, it is important to understand all of the properties of our two-dimensional materials before any real progress can be made in creating new de-

vices.

One metric that is important to understand about a new material is its work function. The work function of a material describes how difficult it is to remove an electron from that material. Work functions are integral to understanding how materials will act electronically, and especially in contact with other materials. For example, if graphene was to be used as a contact to another part of a two-dimensional device, one would need to have an understanding of the work function of both the graphene and the other material to fully realize the energetics required for electrons to move across the boundary.

For two-dimensional devices, these other components often come in the form of other two-dimensional materials. It is possible to make small two-dimensional devices by stacking layers of different two-dimensional materials on top of one another to create what are known as van Der Waals heterostructures, so named because they are held together by van Der Waals forces. van Der Waals forces are relatively weak compared to the strong forces within the plane that hold two-dimensional materials together, leading to a more sandwich type of structure rather than a block of different materials. Since these forces act ubiquitously on two-dimensional materials, different materials can be stacked in any order you could imagine, leading to endless possibilities for device fabrication. [5]

One example of a device that can be made with two-dimensional materials is a field effect transistor, a device that allows current through based on the applied electric field, shown in Figure 1.1. By stacking a two-dimensional semiconductor layer on top of two separate graphene contacts, then placing an insulated graphene contact on top, one can control the field applied to the semiconductor and thus the current passing through the device. [6]

The order materials are stacked is not the only factor to consider. By placing layers of graphene on top of one another with a slight relative twist, you can create a

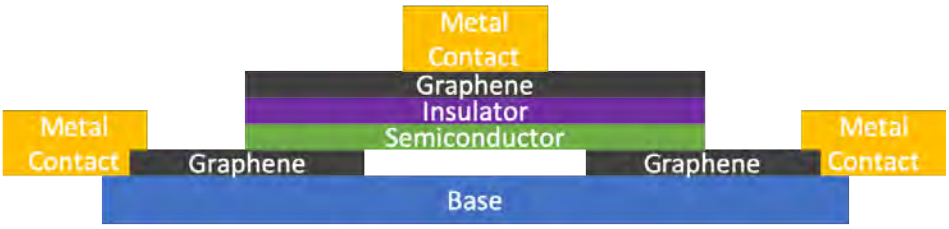

Figure 1.1: An example two-dimensional device known as a field effect transistor.

super-lattice structure known as a Moirè pattern which will be discussed in Section 3.1. These twisted bilayer graphene structures have their own special properties due to the how the individual carbon atoms are positioned in relation to one another between the layers.

In this paper, the work function of three different graphene regimes is studied using Kelvin Probe Force Microscopy (KPFM). This was done using an Asylum Cypher Atomic Force Microscope, pictured below in Figure 1.2 This form of microscopy works by bringing a very small and sharp conducting metal tip close to the sample surface. This tip is on a flexible cantilever, and as it moves and bends due to its interaction with the sample surface a laser pointed at the tip is deflected, allowing measurements to be made to determine both the topography of the sample and its surface potential. In turn, the surface potential is directly related to the work function. The theory behind AFM and KPFM are more extensively discussed in Section 3.2. The results we measure for these samples match well with previous research and provide a promising base on which future research could be conducted.

While this paper focuses on graphene monolayer and bilayer devices, many of the techniques and results will be applicable to understanding other two-dimensional materials and devices structures as well.

Figure 1.2: The AFM used to take measurements in this research.

Chapter 2

Methods

2.1 Fabrication

The fabrication process for twisted bilayer graphene begins with the exfoliation of two-dimensional materials. A small number of crystallites composed of the desired material were placed on a piece of Scotch Tape which was then mechanically exfoliated by repeatedly folding it on itself to cover the tape. Each time the tape was peeled apart, the crystallites were cleaved in half, slowly refining it down toward atomic thickness. This piece of tape would be used as a "master tape". Next, copies would be made by adhering a second piece of tape to the first and slowly peeling it away. The goal here is to create atomically flat regions of each crystal on the tape surface. This would also allow us to use one tape's worth of material to make multiple samples. [7] Graphenium and hexagonal boron nitride (hBN) flakes were also used in this manner to create master tapes.

To find the graphene pieces, material from the exfoliation process would be deposited onto a prepared silicon wafer. The silicon wafer chosen has an oxide layer thickness of 270 nm. This was chosen as the thin film interference between the graphene and the oxide layer at this thickness allowed for the best differentiation between various piece thicknesses under optical microscope. Before use, silicon wafers

would be prepared using a PE25 Plasma Etch system, where they would be placed under vacuum and an oxygen plasma cleaned the surface for 5 minutes. This was done to ensure the surface was as clean as possible before material was deposited.

Once a copy of a master tape was made it would be adhered to a previously prepared piece of silicon wafer. The wafer would be blown off with nitrogen gas just before adhesion to further ensure a clean surface was present. Plastic ended tweezers were used to lightly press the tape down onto the silicon wafer to ensure strong contact was made with the surface.

Once the copy of the master tape was pressed onto the silicon wafer, the wafer was heated for two minutes before being allowed to cool on a cold metal surface for one additional minute. Samples with graphene were heated to 90°C while hBN samples were heated to 130°C.This process was done to promote the adhesion of graphene flakes to the silicon wafer. Once cooled, the tape would slowly be pulled away from the silicon wafer at as low an angle as possible. The tape would then be discarded and the wafer inspected for usable pieces of two-dimensional material.

2.2 Sample Selection

Graphene samples were located optically using a microscope. Exfoliated wafers would be placed under the microscope and scanned at 20x magnification for possibly usable pieces of graphene. An example of a candidate graphene piece is shown below in Figure 2.1. Ideally pieces of graphene would be approximately 40μm square, have little to no contaminants present on or near the sample, and be in a relatively empty area of the wafer. These graphene pieces could be identified as they had a distinctive color due to the thin film interference with the oxide layer. In Figure 2.1 you can see the blue area is bilayer and monolayer graphene while the yellow areas are bulk graphite pieces. There are few enough bulk pieces for this piece to possibly be of use.

If one or two pieces of debris were found nearby a nice piece of graphene, a small

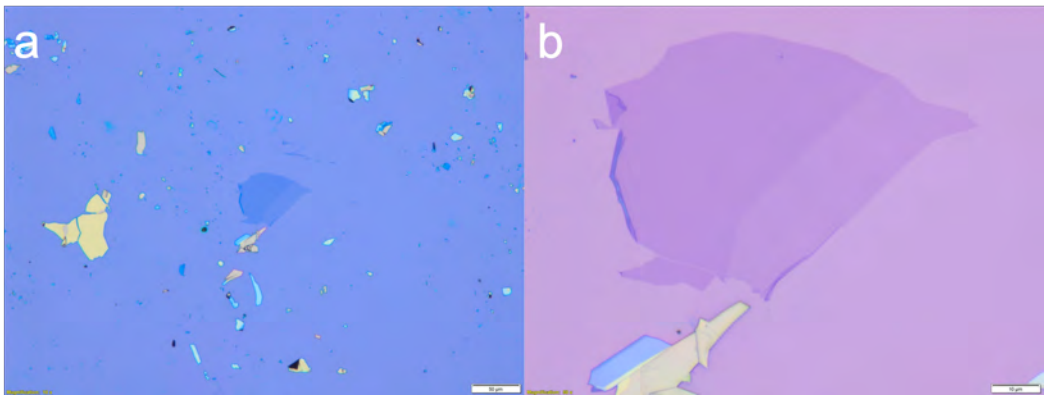

Figure 2.1: Example piece of graphene that may be of use in a device at (a) 20x and (b) 100x magnification.

probe could be used to clear the space. This probe consisted of a sharp metal point mounted to a micro manipulator to allow for fine movement. This point would be brought down to be in contact with the surface then dragged across the wafer to move unwanted pieces away from the sample.

2.3 Stamp Creation

In order to manipulate the two dimensional materials to make our devices, squishy polymer "stamps" were created to stick to and pick up two dimensional materials. The process by which a stamp is made is outlined in Figure 2.3, while the stamp itself is diagrammed in Figure 2.2. A stamp consists of a glass slide onto which a small block of polydimethylsulfate (PDMS) was placed. This block measured approximately 0.25 cm to a side. A thin film of polycarbonate (PC) was stretched over the PDMS and adhered using two-sided tape. The PDMS provides a squishy base to be pressed into the sample while the PC film bonded with the sample to lift it from the wafer. The PC film also has a much lower melting point than the PDMS block, allowing us to use heat to melt this layer off when we want to place down our sample.

In order to create a stamp, first a hole was punched into a piece of double-sided sticky tape and then placed on the end of a glass wafer. A small block of PDMS

approximately 0.5 cm thick was then placed in the center of the hole punched into the tape. The PC film was created by placing a few drops of PC solution onto a glass slide and then quickly placing another glass slide atop the first and swiping away the excess fluid to produce an even film. Once this film dried, a hole was punched into a piece of Scotch Tape and placed on the PC film. Once lifted, the tape would have PC film stretched across the hole punched in the tape. This hole would be lined up with the hole placed in the double-sided sticky tape and placed firmly down so as to stretch the PC film across the PDMS. A diagram of a completed stamp is displayed in Figure 2.2. The stamp making process is then outlined in Figure 2.3.

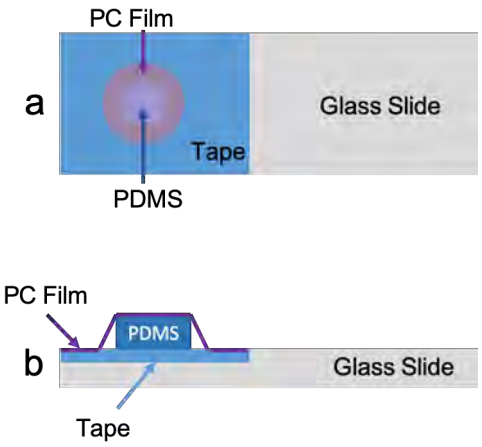

Figure 2.2: Diagram showing the top (a) and side (b) view of the PDMS stamp covered by a thin PC film.

2.4 Material Manipulation

Stamps were maneuvered using a TransferMan NK 2 micro-manipulator in order to place them on top of desired samples. A picture of a mounted stamp is seen in Figure 2.4. A plastic paddle was 3D printed on which glass slides could be mounted so that the manipulator could be used. The glass slide and PDMS are transparent, allowing for an un-obscured image of samples below the stamp. The printed paddle is made of solid ABS plastic and was printed to have a 2 cm square end attached to a

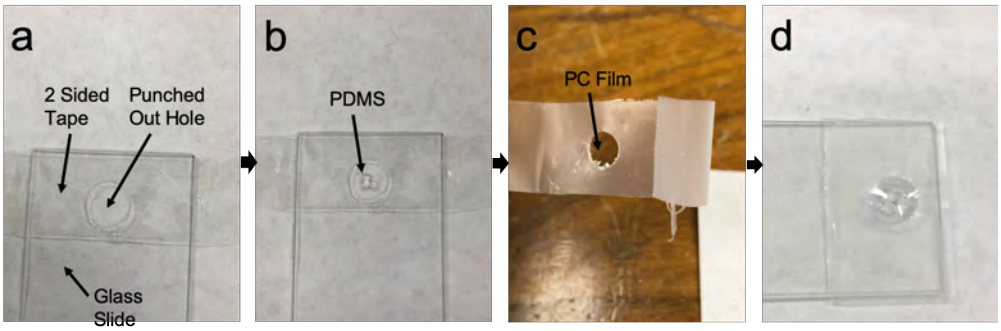

Figure 2.3: Diagram showing the steps in the stamp making process. (a) Tape is initially placed on the glass slide. (b) The PDMS block is then added in the tape hole. (c) A thin PC film is next picked up with a piece of tape, as discussed in the text. (d) Finally the PC is stretched over the PDMS to complete the stamp..

8 cm long arm. The paddle was created because the TransferMan NK 2 is a machine created for precision pipetting, meaning the mount was created to hold pipettes not glass slides.

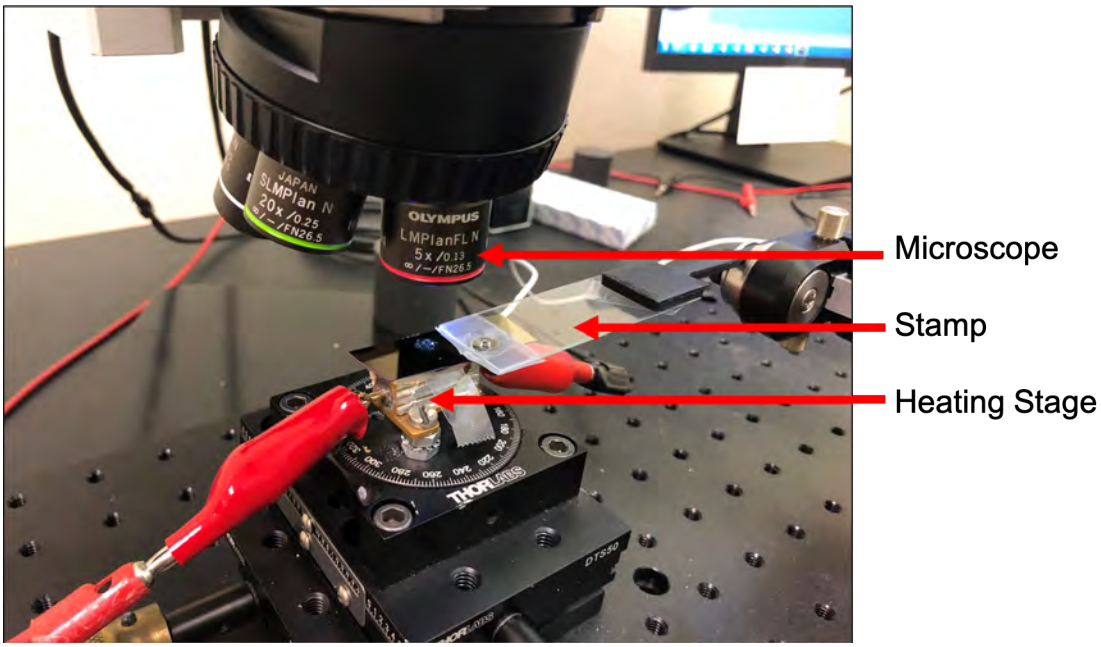

Figure 2.4: Picture of a stamp mounted on the micro-manipulator. The heating stage and microscope are also shown.

The procedure to move a piece of two dimensional material was adapted from Pizzocchero, F. *et al.* and is as follows. [8] Firstly, the silicon wafer is mounted onto

a heating stage using a piece of two sided sticky tape. Then, the target piece was brought into view with our microscope. Once centered, the micro-manipulator would bring in the PDMS stamp to line up the piece with PC film. The stage was heated to 70°C at a rate of 5° per minute before the stamp was slowly brought down onto the sample. Once the desired area was overlapped by the stamp, the stage temperature would be raised to 90°C and then lowered to 40°C before the stamp was slowly pulled up. The temperature is lowered to encourage the material to adhere to the wafer surface rather than the PC film.

For the creation of twisted bilayer devices, a piece of graphene would be ripped by only partly covering the piece with the stamp before picking it up. This would ensure that the resulting relative orientation of the crystal structures was unchanged, allowing for more precise control of the twist angle. [9] The silicon wafer would then be rotated a slight amount before the pickup process was repeated, as shown in Figure 2.5.

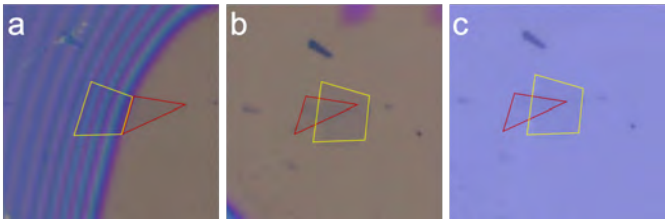

Figure 2.5: A piece of graphene being ripped and made into a twisted bilayer graphene device. The ripping can be seen in (a) where the red piece is picked up. The piece is then placed back down in on the yellow piece as seen in (b). The completed device is shown on the stamp in (c).

After a twisted bilayer device was created, it was placed either on electric contacts or a clean flat hBN surface, depending on the desired measurement. The electrical contacts consist of about 70 nm of gold placed over a few nanometers of vanadium. The vanadium layer helps the gold stick to the silicon oxide layer surface. It was then possible to drape two-dimensional materials over the contacts to allow measurements to be taken. The gold contacts are quite tall compared to the graphene layers, but

this difference in height was not an issue.

To place a finished device on a wafer, the stamp was would be placed down so that the device was in the desired position with the heating stage set to 100°C. Then, the heating stage would be brought up to 180°C so that the PC film would become pliable and begin to lose its structure. At this temperature, the micro-manipulator would wiggle around slightly to attempt to separate the PC film from the stamp, leaving the PC film adhered to the wafer covering the device.

2.5 Cleaning Samples

After the film was detached from the stamp, the wafer would be left to sit for one hour before it would be placed in a chloroform bath to dissolve the PC film. The device would be left in its first chloroform bath for around an hour before it would be transfered to a fresh chloroform bath for three additional hours. While the sample was moved between baths, isopropyl alcohol would be sprayed on the wafer constantly, to prevent any solution from evaporating on top of the device and leaving residue. The goal of this process was to completely remove the PC film from the device, leaving as little residue as possible.

After a device was created it would be optically observed to determine if any contaminants were present. If the device was sufficiently dirty, it would be annealed to attempt to remove any remaining residue. This would be done by placing the sample in a tube furnace with a constant flow of an argon-hydrogen gas blend across the sample to carry away any evaporating material. The furnace would be brought to 400°C while this gas was flowing for a few hours before cooling to room temperature. However, if gold contacts were present, this method was not used so as to not damage the gold contacts.

2.6 Data Collection

The surface potential of samples were measured using Kelvin Probe Force Microscopy (KPFM). A photo of the setup used is shown in Figure 2.6 below. When a sample was going to be placed on gold contacts, these gold contacts were extended using silver paint to ease in the grounding process. After the silver paint dried, silver paint would also be used to adhere the wafer itself onto a magnetic puck that could be mounted into the Cypher AFM. Conductive magnets were then placed on both the silver paint leading to the gold contacts and also on the puck itself. These magnets would then be attached to the ground so that any movement sustained while measuring the sample would not disconnect the wires.

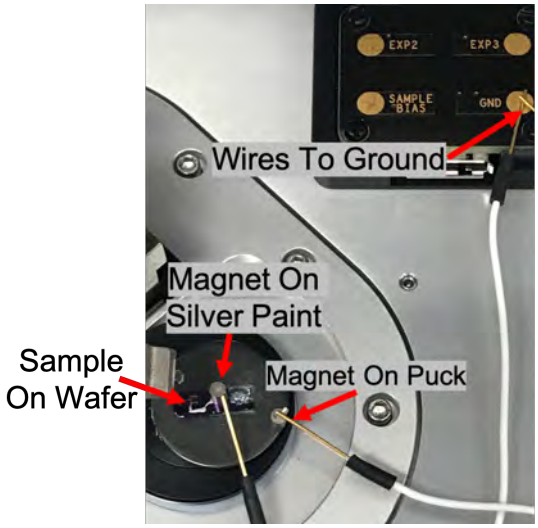

Figure 2.6: A labeled diagram of a sample mounted in an AFM prepared to take surface potential measurements.

Once the sample was loaded into the AFM, tapping mode was used to gather topography and surface potential data. The cantilever tip was automatically tuned by the system with a target amplitude of 1 V. The trigger point for the electric tune was set to 400 mV with the tip being at 3 V. A scan rate of approximately 0.5 Hz was used as slower scan rates allowed for more accurate measurements. More information about this mode can be seen in Section 3.2.

Chapter 3

Theory

3.1 Moirè Patterns

In normal bilayer graphene one expects to see two different types of stacking. These modes are known as AA stacking and AB stacking. In AA stacking (Figure 3.1a), each carbon atom in one lattice is directly above another carbon atom in the lattice below. It is as if each one lattice made a copy of itself directly above its current position. AB stacking (Figure 3.1b) is slightly different, where the second layer is shifted by one lattice position such that a carbon atom from one lattice lies directly in the center of a hexagonal unit of a neighboring lattice. In AB stacking only half of the carbon atoms are directly above one another.

These are the two types of stacking one might find occurring naturally as they are both very regular and have stable lattices. However, each of them displays slightly different electrical properties because electrons are more easily able to hop between layers in AA stacked graphene. [10] One consequence of this is that AA stacked graphene has a higher conductivity than AB stacked graphene. [11]

It is also possible to artificially stack graphene. Then the layers could theoretically be stacking any way, including with a small twist angle between each layer. This will generate what is known as a "Moirè Pattern", a super-lattice structure that is

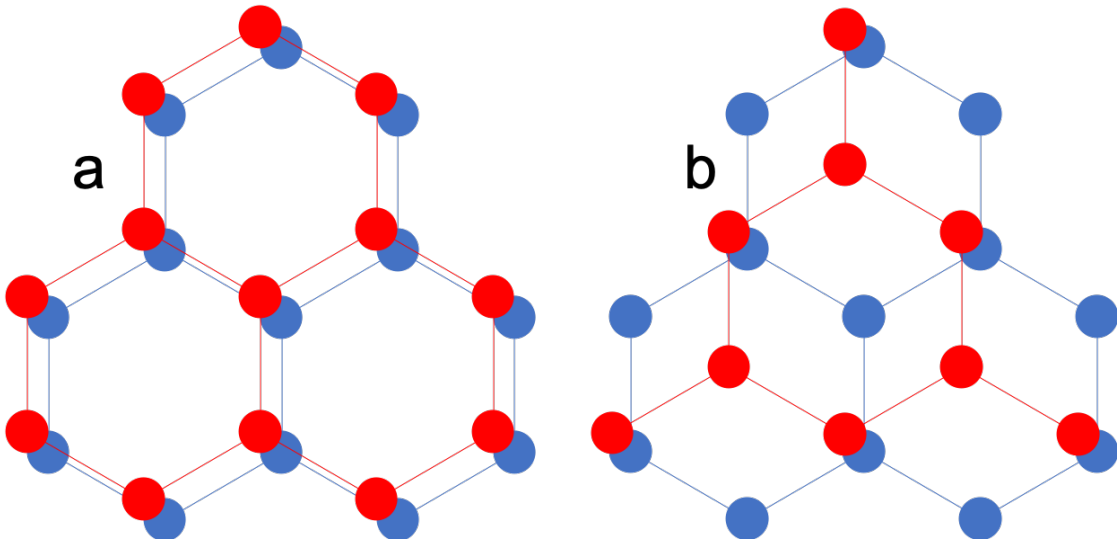

Figure 3.1: Diagram showing AA (a) and AB (b) stacking types.

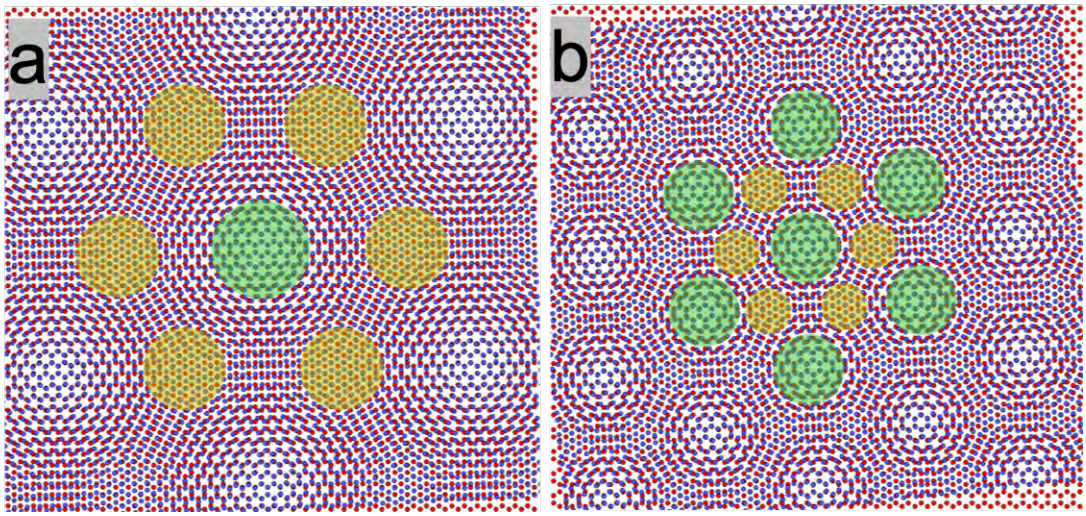

Figure 3.2: A diagram of a graphene bilayer displaying a Moirè Pattern with a twist angle of (a) 5°and (b) 10°. AA stacked regions are marked in green and AB stacked regions are marked in yellow.

apparent when viewed from a distance. An example of this effect in graphene is shown in Figure 3.2.

As you can see, when a Moirè Pattern is created, the graphene bilayer exhibits a mixing of AA and AB stacking. This mix of stacking occurs with its own hexagonal crystal structure, and leads to unique behaviors. As shown in Figure 3.2, if the twist angle increases, the period of the super-lattice structure of AA and AB regions gets

smaller. This size continues to decrease as the twist angle approaches 30°, where the period is the smallest. By hexagonal the symmetry of graphene a 60°rotation is equivalent to no rotation at all (0°),

This super-lattice structure affects not only the geometric properties of the graphene, but also the electrical ones. The mixing of AA and AB stacking regions leads to interesting electric properties that depend heavily on twist angle. For large twist angles, there is little change from what is seen in AA stacking. This is because when the twist angle is large enough, the two graphene layers "decouple" and begin to act as two separate graphene sheets. However, at small twist angles new properties begin to appear, such as the discovery of superconductivity at a "magic angle" of approximately 1.5°. [12] In general, small twist angles lead to the most interesting behavioral changes.

Twist angle can be hard to determine as a device is being created. Precisely controlling the angle is difficult to do in lab and even if you know the exact angle, it is possible the graphene will shift slightly as it is placed down onto another layer or during other processing steps. To solve this problem, the following equation could be used to determine the twist angle from a two-dimensional image by measuring the period of the Moirè pattern L using an AFM. [13]

$$L = \frac{a_0\sqrt{3}}{2sin(\theta/2)} \tag{3.1}$$

With $a_0 = 1.1$Å and $\theta \leq 30°$.

The period of the Moirè pattern can be determined by measuring the distance between the AA stacking regions. It is possible to see the different stacking types under electron or probe microscopy if the sampled region is quite clean and the microscope is isolated from outside vibration.

3.2 AFM Theory

In the Cypher AFM, tapping mode was used to gather all the necessary data. In general, atomic force microscopy works by using a sharp probe on a cantilever to measure the topography of the sample. A small diagram showing this probe is shown in Figure 3.3. In tapping mode, this sharp point is made to resonate above the sample before slowly being brought down toward the surface. As the tip begins to engage with the surface, the amplitude and frequency of these oscillations changes due to the force acting on the probe. A laser pointed at the back of the oscillating cantilever can monitor this change in frequency and determine at which point the tip actually makes contact with the sample, giving topography data. This tapping can be rastered across a sample to get a full image of the topography.

Other measurements that can be taken in this tapping mode are phase measurements and surface potential measurements. Phase measurements are taken by determining how the phase of the taps changes when the tip comes into contact with the surface. If a tip comes into contact with a perfectly elastic surface the phase will not change much. However, when the tip comes into contact with a more pliable surface, it will shift in phase as it sticks to the surface each tap. These phase measurements are useful in determining changes in material where the change in topography is more difficult to see.

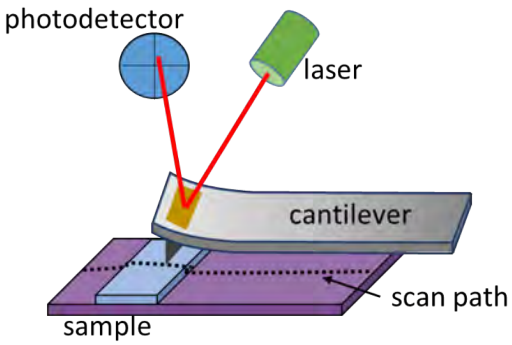

Figure 3.3: A schematic of the atomic force microscope cantilever motion and detection. Image used with permission.

The surface potential of various samples can be measured using KPFM. By using a conducting tip inside of an atomic force microscope, one can measure the potential difference between the probe and the sample when the two come into contact. This voltage is defined as follows. [14]

$$V_{CPD} = \frac{\phi_{tip} - \phi_{sample}}{-e} \tag{3.2}$$

Where ϕ represents the work function. This voltage is created when the tip comes into contact with the sample and an electronic equilibrium is established between the tip and the sample.

Previous research has shown that under atmospheric conditions, the difference in surface potential between monolayer and bilayer graphene is approximately 35 mV, though when the surface is cleaned and treated with N_2 gas no difference in work function was observed. [15] A difference was also observed between monolayer graphene and twisted bilayer graphene, where it is theorized that the work function undergoes changes of the similar magnitude as the relative twist angle is changed. [16]

Chapter 4

Results and Analysis

4.1 Results

Surface potential measurements were taken for three different samples on an Cypher Atomic Force Microscope using tapping mode KPFM. The first sample measured was a twisted bilayer graphene sample placed on an hBN substrate. The surface potential difference between the monolayer and twisted bilayer regions of the sample was found to be approximately 21 mV, as displayed in Figure 4.1.

There is a clear boundary between the hBN and graphene layers visible in topography, but the boundary between the monolayer and twisted bilayer sections of the graphene is obscured by the imperfections in the surface. However, the surface potential plot more clearly shows off the three regions. These three regions were used to create the histogram in (c) which illustrates the difference in surface potential quantitatively. Each material has an average peak surface potential value, and comparing them gives the aforementioned 21 mV.

The second sample measured was a bilayer piece of graphene placed on gold contacts. The surface potential difference measured between the bilayer graphene and the gold was approximately 20 mV as displayed in Figure 4.2. The area measured for this sample's histogram is also included in Figure 4.3. In order to make the best

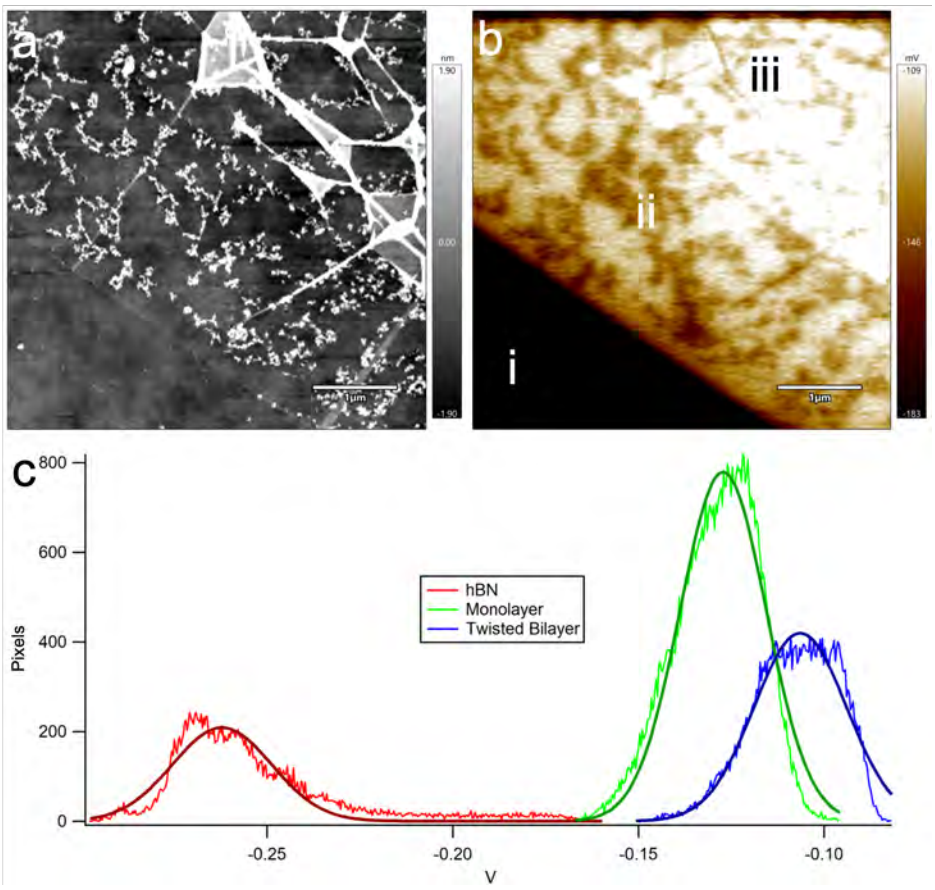

Figure 4.1: KPFM data for the twisted bilayer graphene sample on hBN. (a) Topography (b) Surface Potential, taken in parallel. Labeled regions are (i) hBN, (ii) monolayer graphene, and (iii) twisted bilayer graphene. (c) Histogram of potential values for each pixel overlaid with Gaussian fit.

possible comparison, only areas very close to the bilayer sample were considered for the gold contact histogram creation. Likewise, only graphene on the gold contact was considered for the creation of the bilayer histogram. However, when the entirety of the available space is sampled, the results are not significantly different. This does however reduce the height of the histogram when compared to the first sample.

Due to the horizontal nature of the scan, the boundary between the gold contact and silicon wafer is somewhat obscured. However, the difference between the bilayer graphene and gold contact is quite clear on both the topography and potential scans.

The final sample measured was a monolayer piece of graphene placed on a gold contact. During the process of placing the piece down on the contact, it ripped into

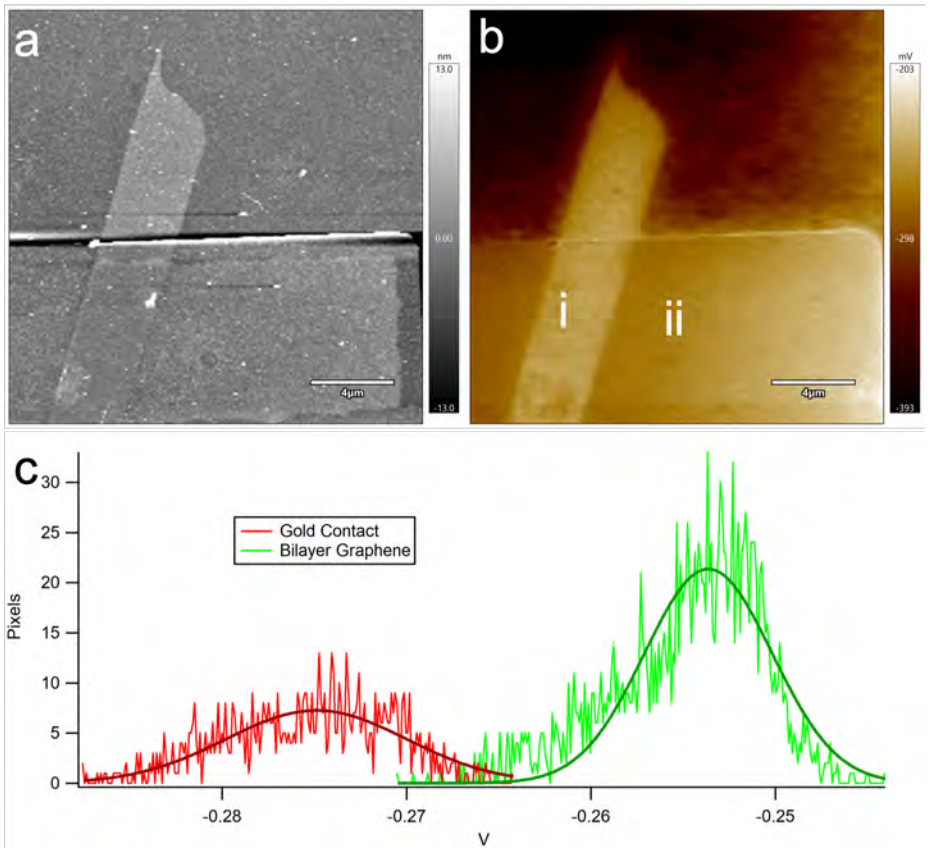

Figure 4.2: KPFM data for the bilayer graphene sample on gold contacts. (a) Topography (b) Surface Potential, taken in parallel. Labeled areas are (i) bilayer graphene and (ii) gold contact. (c) Histogram of potential values for each pixel overlaid with Gaussian fit.

two pieces, splitting the monolayer. However, there is still monolayer graphene placed down on the contact, as can be seen in Figure 4.4 below. The surface potential scan is somewhat damaged by what seems to be contamination picked up during the scanning process, there are some scan lines where there is consistent readings in which the gold and monolayer surface potentials can be directly compared. A line cut of potential has been taken in this region showing an approximate 30 mV difference. A line cut was used as there was not enough area available to make a meaningful histogram.

For this sample, the phase is shown as the boundary between the monolayer graphene and the contact is difficult to see. This is because in the topography scan the image is scaled to best show the boundary between the gold contact and the silicon

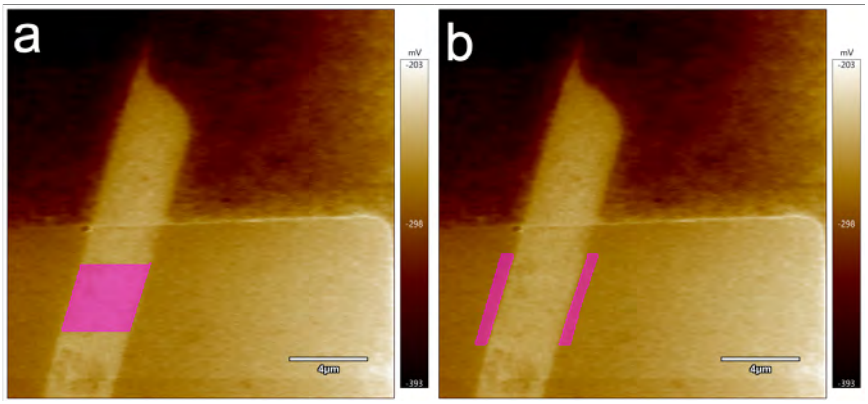

Figure 4.3: Diagram showing the different regions sampled to create the histogram shown in Figure 4.2 highlighted in pink. Region (a) is the area sampled for the bilayer region while region (b) is the area sampled for the gold contact region.

wafer which is much taller than the graphene height. The phase however is unaffected by this large height difference and still clearly shows the two different region types.

An interesting phenomenon seen here is that the edges of the graphene sample seem to have different potential values than the center. This is seen not only in the graphene on the gold contact, but also on the graphene placed on the silicon wafer.

4.2 Analysis

From the data gathered, the difference between in surface potential of monolayer and bilayer graphene is measured to be 50 mV. This can be calculated by using the gold contact as a reference point. Note we add the two measured $\Delta\phi$ values because the monolayer surface potential is below that of the gold contact but the bilayer surface potential is above the gold contact zero point. This result is in line with previous results, lying between previously measured values of 35 mV [15], 66 mV [17], and 126 mV. [16] It is possible that the contamination of the probe in the monolayer measurement may have had an overall effect on the measured surface potential in some meaningful way. It is also possible that the devices constructed in other papers, measuring the bilayer surface potential and monolayer surface potential on the same

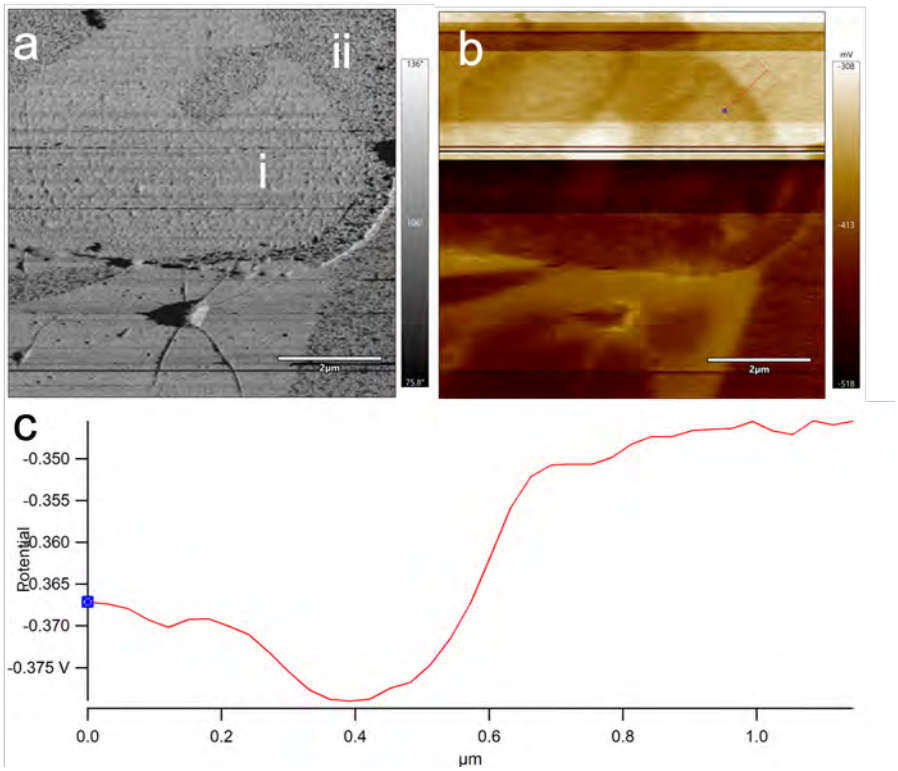

Figure 4.4: KPFM data for the monolayer graphene sample on gold contacts. (a) Phase (b) Surface Potential, taken in parallel. Labeled areas are (i) monolayer graphene and (ii) gold contact. (c) Line cut of potential values across the region shown in (b).

scan, could lead to different values than taking the two measurements separately on gold contacts.

The other significant data point derived from these measurements is that the difference in surface potential between monolayer and twisted bilayer graphene 20 mV. Previous results show that for a 16°twist angle there was a decrease from a 126 mV surface potential difference between monolayer and bilayer graphene to a 91 mV surface potential difference between monolayer graphene and the twisted bilayer graphene. [16] These values are similar to what was observed in that a twist angle being introduced reduced the difference in surface potential, but the magnitude of the change is much larger in our observed data. This discrepancy may be in part due to our sample being mechanically constructed rather than chemically grown as was done in

the compared study. This difference may introduce more or fewer impurities and possibility for error. It also might result from a difference in twist angle, as we are unable to determine what the twist angle of our sample is. Regardless, potential difference between monolayer and twisted bilayer pieces matches with the accepted theory that as twist angle increases, the graphene layers become decoupled and begin to act more as two separate single layers, bringing the work function closer to that of monolayer graphene.

Chapter 5

Conclusion

In conclusion, our measurements of monolayer, bilayer, and twisted bilayer graphene surface potentials are consistent with values obtained in previous experiments. [15, 16, 17] These results, showing differences in potential of 50 mV between monolayer and bilayer graphene and 20 mV between monolayer and twisted bilayer graphene, are promising first steps into future research with twisted bilayer graphene. Understanding the work function is a first step toward more complex analysis of graphene and its potential uses. In the future, goals would be to understand the presence and reduce the impact of contamination, determine how certain cleaning methods effect the surface potential measurements, and develop a better relationship between specific twist angles and surface potentials.

References

[1] The Nobel Prize in Physice 2010, 2010.

[2] C. Lee, X. Wei, J. W. Kysar, and J. Hone, Science **321**, 385 (2008).

[3] A. K. Geim and K. S. Novoselov, Nature Materials **6**, 183 (2007).

[4] Y. Cao, V. Fatemi, S. Fang, K. Watanabe, T. Taniguchi, E. Kaxiras, and P. Jarillo-Herrero, Nature **556**, 43 (2018).

[5] A. K. Geim and I. V. Grigorieva, Nature **499**, 419 (2013).

[6] F. Giannazzo, G. Greco, F. Roccaforte, and S. S. Sonde, Crystals **8**, 70 (2018).

[7] P. V. Nguyen, N. C. Teutsch, N. P. Wilson, J. Kahn, X. Xia, V. Kandyba, A. Barinov, G. Constantinescu, N. D. M. Hine, X. Xu, D. H. Cobden, and N. R. Wilson, (2019).

[8] F. Pizzocchero, L. Gammelgaard, B. S. Jessen, J. M. Caridad, L. Wang, J. Hone, P. Bøggild, and T. J. Booth, Nature Communications **7**, 11894 (2016).

[9] K. Kim, A. DaSilva, S. Huang, B. Fallahazad, S. Larentis, T. Taniguchi, K. Watanabe, B. J. LeRoy, A. H. MacDonald, and E. Tutuc, Proceedings of the National Academy of Sciences **114**, 3364 (2017).

[10] A. Rozhkov, A. Sboychakov, A. Rakhmanov, and F. Nori, Physics Reports **648**, 1 (2016), electronic properties of graphene-based bilayer systems.

[11] M. Ould Ne, M. Boujnah, A. Benyoussef, and A. El Kenz, Journal of Superconductivity and Novel Magnetism **30**, (2016).

[12] E. Suárez Morell, J. D. Correa, P. Vargas, M. Pacheco, and Z. Barticevic, Phys. Rev. B **82**, 121407 (2010).

[13] Z. Y. Rong and P. Kuiper, Phys. Rev. B **48**, 17427 (1993).

[14] W. Melitz, J. Shen, A. C. Kummel, and S. Lee, Surface Science Reports **66**, 1 (2011).

[15] R. Pearce, J. Eriksson, T. Iakimov, L. Hultman, A. Lloyd Spetz, and R. Yakimova, ACS Nano **7**, 4647 (2013), pMID: 23631346.

[16] J. T. Robinson, J. Culbertson, M. Berg, and T. Ohta, Scientific Reports **8**, 2006 (2018).

[17] D. Ziegler, P. Gava, J. Güttinger, F. Molitor, L. Wirtz, M. Lazzeri, A. M. Saitta, A. Stemmer, F. Mauri, and C. Stampfer, Phys. Rev. B **83**, 235434 (2011).